Biochimica et Biophysica Acta 1807 (2011) 471–481

Contents lists available at ScienceDirect

Biochimica et Biophysica Acta

journal homepage: www.elsevier.com/locate/bbabio

Molecular environments of divinyl chlorophylls in *Prochlorococcus* and *Synechocystis*: Differences in fluorescence properties with chlorophyll replacement

Mamoru Mimuro [a,*], Akio Murakami [b], Tatsuya Tomo [c], Tohru Tsuchiya [a], Kazuyuki Watabe [a], Makio Yokono [d], Seiji Akimoto [d,e,**]

[a] *Graduate School of Human and Environmental Studies, Kyoto University, Kyoto 606-8501, Japan*
[b] *Kobe University Research Center for Inland Seas, Awaji 656-2401, Japan*
[c] *Department of Biology, Faculty of Science, Tokyo University of Science, Kagurazaka 1-3, Shinjuku-ku, Tokyo 162-8601, Japan*
[d] *Molecular Photoscience Research Center, Kobe University, Kobe 657-8501, Japan*
[e] *JST, CREST, Kobe 657-8501, Japan*

ARTICLE INFO

Article history:
Received 9 August 2010
Received in revised form 22 February 2011
Accepted 28 February 2011
Available online 4 March 2011

Keywords:
Cyanobacteria
Divinyl chlorophyll
Evolution
Fluorescence
Photosynthesis
Time-resolved spectroscopy
Prochlorococcus

ABSTRACT

A marine cyanobacterium, *Prochlorococcus*, is a unique oxygenic photosynthetic organism, which accumulates divinyl chlorophylls instead of the monovinyl chlorophylls. To investigate the molecular environment of pigments after pigment replacement but before optimization of the protein moiety in photosynthetic organisms, we compared the fluorescence properties of the divinyl Chl *a*-containing cyanobacteria, *Prochlorococcus marinus* (CCMP 1986, CCMP 2773 and CCMP 1375), by a *Synechocystis* sp. PCC 6803 (*Synechocystis*) mutant in which monovinyl Chl *a* was replaced with divinyl Chl *a*. *P. marinus* showed a single fluorescence band for photosystem (PS) II at 687 nm at 77 K; this was accompanied with change in pigment, because the *Synechocystis* mutant showed the identical shift. No fluorescence bands corresponding to the PS II 696-nm component and PS I longer-wavelength component were detected in *P. marinus*, although the presence of the former was suggested using time-resolved fluorescence spectra. Delayed fluorescence (DF) was detected at approximately 688 nm with a lifetime of approximately 29 ns. In striking contrast, the *Synechocystis* mutant showed three fluorescence bands at 687, 696, and 727 nm, but suppressed DF. These differences in fluorescence behaviors might not only reflect differences in the molecular structure of pigments but also differences in molecular environments of pigments, including pigment–pigment and/or pigment–protein interactions, in the antenna and electron transfer systems.

1. Introduction

Prochlorococcus forms a unique taxonomic group within cyanobacteria [1,2], in which the organism accumulates divinyl (DV) chlorophylls (Chls) instead of the monovinyl (MV) form that is commonly found in almost all cyanobacteria, all algae, and plant [1]. As the Soret bands of DV-Chl *a* and DV-Chl *b* shift to the red by approximately 10 nm compared to those of MV-Chl *a* and MV-Chl *b*, respectively, *Prochlorococcus* has an advantage over coexisting *Synechococcus*, which contains MV-Chl *a* and phycobiliproteins, in absorbing blue light in deep water in the oceans [3]. The evolutionary modification is due to the lack of 3,8-divinyl protochlorophyllide *a* 8-vinyl reductase in the MV-Chl biosynthesis pathway [4]. Disruption of a gene encoding this enzyme in *Synechocystis* sp. PCC 6803 (hereafter referred to as *Synechocystis*) resulted in the change of all Chl pigments to their DV form alike *Prochlorococcus* [5,6]. The primary electron acceptor of photosystem (PS) II, pheophytin *a* (Phe *a*), might also take the DV form if Phe *a* is synthesized from Chl *a* [7]. By changing pigment composition, *Prochlorococcus* has capacity to adapt the antenna complexes to light variations; pigment ratios of DV-Chl *b*/DV-Chl *a* and zeaxanthin/DV-Chl *a* change depending on light conditions [8].

Prochlorococcus is frequently found in the oligotrophic ocean in tropical and subtropical regions and is the major primary producers in these areas [9,10]. More than 30 strains have been isolated, and of these, the genomes of 12 strains have been sequenced [11; http://genome.kazusa.or.jp/cyanobase]. Based on this genomic information, an evolutionary pathway(s) and/or a species differentiation process

Abbreviations: Chl, chlorophyll; DF, delayed fluorescence; DV, divinyl; FWHM, full width at the half maximum; MV, monovinyl; PS, photosystem; TRFS, time-resolved fluorescence spectrum; WT, wild type; FDAS, fluorescence decay-associated spectrum

* Corresponding author.
** Correspondence to: S. Akimoto, Molecular Photoscience Research Center, Kobe University, Kobe 657-8501, Japan. Tel./fax: +81 78 803 5705.
E-mail address: akimoto@hawk.kobe-u.ac.jp (S. Akimoto).

0005-2728/$ – see front matter © 2011 Elsevier B.V. All rights reserved.
doi:10.1016/j.bbabio.2011.02.011

(es) for a specific group of cyanobacteria, marine *Synechococcus* to *Prochlorococcus*, has been discussed [12,13]. According to the 16S rDNA sequence, these two genera, with only a short genetic distance between them, were derived from a common ancestral cyanobacterium [2]. The evolutionary process(es) has also been discussed in terms of genome size [14]. The marine *Synechococcus* sp., WH7803 has a genome of approximately 2.37 Mb with 2586 genes [10; http://genome.kazusa.or.jp/cyanobase]. On the other hand, *Prochlorococcus* shows greater diversity in genome size; for example, the *P. marinus* strain, MIT 9303, has a relatively large genome (2.68 Mb with 3049 genes), while the *P. marinus* strain, MED4, has lost a significant part of its genome (1.66 Mb with 1756 genes) compared with *Synechococcus*.

The process(es) involved in the reduction of genome size is hypothesized based on their residual sequences [14]. Primary photochemical reactions in photosynthesis are carried out in pigment–protein complexes, such as antenna complexes and reaction center complexes. Pigments in these complexes are correctly localized through pigment–protein and/or pigment–pigment interactions. When the interaction is less strict, pigments, especially Chls, sometimes form radical species that are harmful for the component–proteins, which eventually leads to damage of the photochemical reaction systems. It has been clearly demonstrated that the yield of singlet oxygen by DV-Chl *a* is approximately 20% higher than that from MV-Chl *a* in an acetone solution [15]. Therefore, interactions between pigments, and/or between pigments and proteins, are critical for the stabilization of reaction systems. The replacement of pigment species may cause instability within the system. One such example has been observed in reconstituted pigment–protein complexes [16]. The stoichiometry in the reconstituted complexes is different from that in natural complexes, such that the binding of pigments to the protein moiety is not necessarily accurately reproduced [16], and this leads to artificial reaction(s).

When we consider the evolutionary processes accompanied by pigment modifications, it is reasonable to assume that an exchange in pigment may occur due to a mutation in one or a small number of genes encoding biosynthetic enzymes; however, it may take a long time for the accompanying changes in protein moieties to reach optimal conditions with the new pigment. It is very difficult, or impossible, to find a species that shows an intermediate state (in other words, a state in which the pigment has been replaced but the protein is not yet optimized by substitution in amino acid residues); therefore, to investigate differences in energy transfer and primary electron transfer processes caused by the pigment replacement before the optimization process(es), we compared *P. marinus* with a *Synechocystis* mutant whose pigment was replaced with DV-Chl *a* [5,6].

It is known that *Prochlorococcus* is hard to grow at high density under laboratory culture conditions. This is a major problem when analyzing the fundamental properties of photosynthesis in this species. Therefore, we improved a method for growing three typical strains of *P. marinus*, namely *P. marinus* CCMP 1986 (isolated from the eastern Mediterranean Sea, at a depth of 5 m, by Vaulot and Partensky) [http://ccmp.bigelow.org/], *P. marinus* CCMP 2773 (from the Gulf Stream, at a depth of 135 m) [http://ccmp.bigelow.org/], and *P. marinus* CCMP 1375 (isolated from the deep euphotic zone of the Sargasso Sea by Palenik) [17; http://ccmp.bigelow.org/]. We then compared their optical properties with the DV-Chl *a*-containing mutant of *Synechocystis* as the first step in our analysis of the optimization process(es) after replacement of a pigment. Although the fluorescence properties of *Prochlorococcus* have already been partially reported [18–21], we investigated this property primarily in conjunction with time-resolved fluorescence spectroscopy (TRFS) because fluorescence spectra preferentially reflect the molecular environment of pigments. We used intact cells to avoid any artifacts introduced by sample preparations. Based on our findings, we discuss the molecular environments of the pigments following replacement of a photosynthetic pigment, MV-Chl to DV-Chl.

2. Materials and methods

2.1. Algal culture

Three strains of *P. marinus*, CCMP 1986 (MED4), CCMP 2773 (MIT9313) and CCMP 1375 (SS120), were purchased from the Provasoli-Guillard National Center for the Culture of Marine Phytoplankton (Maine, USA) and were cultured autotrophically in Pro99 medium following the distributor's recommendations. The light intensity of the fluorescent lamp was adjusted depending on the species: 40 μmol photons m^{-2} s^{-1} were used for the high-light adapted strain (*P. marinus* CCMP 1986), which was reduced to 4 μmol photons m^{-2} s^{-1} for the low-light adapted strains (*P. marinus* CCMP 2773 and *P. marinus* CCMP 1375). A light–dark regime was applied (12 h light:12 h dark), and the temperature was kept at 293 K. Culture bottles were placed in the incubator and were not shaken mechanically. Wild-type (WT) and a DV-Chl *a*-containing mutant of *Synechocystis* sp., PCC 6803 were grown in BG11 medium under continuous white light illumination (20 μmol photons m^{-2} s^{-1}) at 298 K [22].

2.2. Spectroscopy

Absorption and fluorescence spectra were measured using a Hitachi 557 spectrophotometer and a Hitachi 850 spectrofluorometer, respectively [22]. To assess the low-temperature absorption spectrum, the Hitachi 557 was used with a custom-made Dewar bottle. For the low-temperature fluorescence spectrum (77 K), a home-made Dewar bottle was used, and polyethylene glycol (PEG, average molecular weight 3350, final concentration 15% (w/v), Sigma-Aldrich) was added to obtain homogeneous ice nucleation. The spectral sensitivity of the fluorometer was corrected using a substandard lamp with a known radiation profile. The excitation spectrum was not corrected. TRFS and fluorescence decay curves were measured using time-correlated single-photon counting methods [23] with an excitation wavelength of 425 nm (the second harmonic of the 850 nm oscillation). The repetition rate of the excitation pulse was 2.9 MHz. The fluorescence lifetime was estimated using a convolution calculation [23]. The spectral and time resolutions for TRFS were 1 nm/channel and 1.2 ps/channel, respectively.

2.3. Pigment analysis

Pigment composition was analyzed based on the method described by Zapata et al. [24]. Pigments were extracted from cells with cold methanol, and deionized water was added to a final concentration of 20%. The pigments were then immediately analyzed by high-performance liquid chromatography (HPLC; Prominence series, Shimadzu, Kyoto, Japan) with a Symmetry C8 column (150 × 1.0 mm, 3.5 μm particle size; Waters, MA, USA). The elution profile was monitored with a photodiode array detector (SPD-M20A, Shimadzu, Japan). The compositions of the mobile phases were methanol/acetonitrile/0.25 M pyridine solution (50:25:25, v/v/v) and methanol/acetonitrile/acetone (20:60:20, v/v/v), and a gradient profile was optimized for semi-micro analysis.

2.4. Oxygen-evolving activity

Oxygen-evolving activity was measured using a Clark-type oxygen electrode (Rank Brothers, England) at 293 K under continuous saturating white light (approximately 600 μmol photons m^{-2} s^{-1}). *P. marinus* cells were harvested by centrifugation (15,000 × *g*, 20 min) and re-suspended in new medium. Following 10 min of dark adaptation, the oxygen-evolving activity was recorded. The Chl concentration was adjusted to approximately 10 μg ml^{-1}; however, the actual concentration in individual batches was estimated by

methanol extraction and optical measurements with a Hitachi 340 spectrophotometer and using the extinction coefficient reported by Porra et al. [25].

3. Results

3.1. Growth of the three strains of P. marinus

Growth rates were estimated by measuring the increase in Chl concentration. The growth rate constants (μ) were 0.51, 0.07, and 0.13 day^{-1} for *P. marinus* CCMP 1986, *P. marinus* CCMP 2773, and *P. marinus* CCMP 1375, respectively. These values were much lower than that observed for *Synechocystis* (approximately 1.0 day^{-1}), irrespective of the pigment species, MV- or DV-Chl *a* measured (data not shown).

For an index of physiological activity, we measured the oxygen-evolving activity under saturating white light. The activities were 1330, 255, and 495 μmol O_2 (mg Chl)$^{-1}$ h^{-1} for *P. marinus* CCMP 1986, *P. marinus* CCMP 2773, and *P. marinus* CCMP 1375, respectively. The light intensity that gave the maximum activity was different for each strain, and was higher for the high-light adapted strain. Compared with the activity of the DV-Chl *a Synechocystis* mutant (approximately 400 μmol O_2 (mg Chl)$^{-1}$ h^{-1}) [26], the value recorded for *P. marinus* CCMP 1986 (1330 μmol O_2 (mg Chl)$^{-1}$ h^{-1}) was much higher. This was the most striking value so far reported in intact cells of cyanobacteria. Even for the low-light adapted strains, the oxygen-evolving activity of *P. marinus* was not low.

3.2. Pigment composition

Four major pigments, DV-Chl *a*, DV-Chl *b*, α-carotene and zeaxanthin were identified in the three strains of *P. marinus* by HPLC analysis (see Fig. S1 in Supporting Information) and from absorption spectra on a photodiode array detector (data not shown). In addition, a Chl *c*-like pigment was also detected at the retention time of 14.5 min. This pigment composition is basically similar to that reported previously [27], although the relative amounts of these pigments varied depending on both the strain and culture conditions, such as light intensity and light quality [27]. With respect to the carotenoids, α-carotene was the major component found in the three strains under our culture conditions, accounting for more than half of the total carotenoids. The carotenoid content relative to Chl *a* was also variable depending on the strain. The pigment content of the high-light adapted strain, *P. marinus* CCMP 1986, did not change significantly even under low-light culture conditions (data not shown).

3.3. Variations in absorption spectra with respect to replacement of Chl

The absorption spectra of *Synechocystis* at 80 K are shown in Fig. 1A. For the MV-Chl *a*-containing WT, several peaks were resolved for the Qy transition of Chl *a*, together with phycocyanin, at approximately 630 nm, and for the carotenoids at approximately 460 nm to 510 nm. Red Chls were clearly detected in the wavelength region longer than 700 nm. In the case of DV-Chl *a*-containing mutant, a red-shift of approximately 7 nm was clearly observed for the Soret band; however, there was almost no change in the Qy region. Red Chls were also detected.

The absorption properties of the three strains of *P. marinus* were resolved in much greater detail by measurements at 80 K (Fig. 2A). The Qy band of DV-Chl *a* was resolved to several component bands for each of the three species through analyses of the second derivative spectrum (Table 1). *P. marinus* CCMP 1986 showed what looked like one peak but was resolved to four peaks of 669.0 nm, 678.5 nm, 686.0 nm and 699.5 nm (Table 1); of these, the 669 nm peak was highest. A carotenoid band was resolved at 501.0 nm (data not shown). *P. marinus* CCMP 2773 produced four DV-Chl *a* peaks at

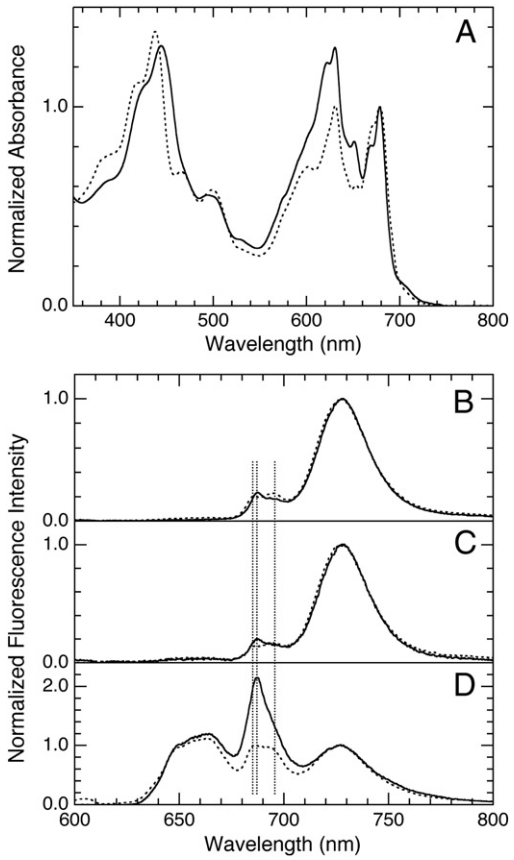

Fig. 1. Normalized absorption and steady-state fluorescence spectra for WT (dotted lines) and DV-Chl *a*-containing *Synechocystis* sp. PCC6803 (solid lines). (A) Absorption spectra at 80 K. (B, C, D) Fluorescence spectra at 77 K. Excitation wavelengths are 435 nm (B), 500 nm (C), and 580 nm (D). Vertical lines locate at 685, 687, and 696 nm.

670.0 nm, 676.0 nm, 685.0 nm and 700.0 nm, and their locations were almost identical to those of *P. marinus* CCMP 1986. In addition to these DV-Chl *a* bands, 650.0-nm and 657.5-nm bands from DV-Chl *b* were also evident. Red Chls were also detected at 700.0 nm. The carotenoid band was shifted to the red by 15 nm compared with the peak of *P. marinus* CCMP 1986 (Fig. 2A). In the case of *P. marinus* CCMP 1375, the main band was the DV-Chl *b* band at 655.0 nm, and three DV-Chl *a* bands were resolved at 674.0 nm, 683.5 nm and 700.5 nm. All three strains showed a small, but significant, band at approximately 700 nm, which suggested the presence of red Chls in *Prochlorococcus*.

3.4. Steady-state fluorescence spectra

Upon excitation of Chl *a* at 435 nm, *Synechocystis* WT (Fig. 1B) showed three fluorescence maxima at 685 nm, 696 nm and 727 nm at 77 K from PS II Chl *a*, PS II Chl *a*, and PS I Chl *a*, respectively. In contrast, the *Synechocystis* mutant containing DV-Chl *a* (Fig. 1B) showed a clear red-shift of the PS II fluorescence to 687 nm and a relatively low intensity for the 696-nm band, indicating that the energy transfer from the 687-nm component to the 696-nm component was somewhat suppressed. The lower efficiency was much enhanced by the excitation of phycocyanin at 580 nm. The difference in the energy transfer efficiency between the WT and the DV-Chl *a* mutant was remarkable.

The fluorescence spectra for the three strains of *P. marinus* (Fig. 2B–D) were very different from those of the DV-Chl *a*-containing *Synechocystis* mutant (Fig. 1B–D). At 77 K, the three strains of *P. marinus* showed spectra with a single peak at approximately 687 nm, and no indication of a PS I band even after the second derivative

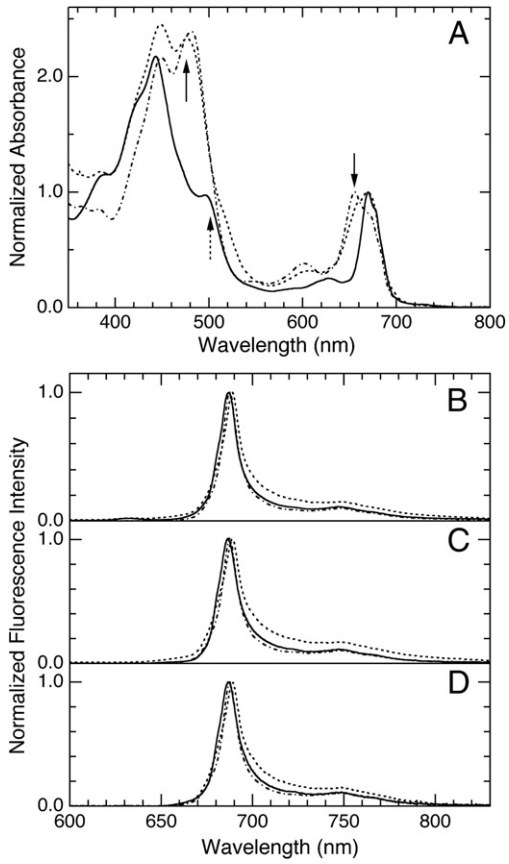

Fig. 2. Normalized absorption at 80 K and steady-state fluorescence spectra at 77 K for three strains of *P. marinus* CCMP 1986 (solid lines), CCMP 2773 (dotted lines), and CCMP 1375 (dash-dotted lines). (A) Absorption spectra at 80 K. Vertical arrows show peaks of Chl *b* (solid line) and carotenoid (dotted line). Precise peak wavelengths are described in the text. (B, C, D) Fluorescence spectra at 77 K. Excitation wavelengths are: 445 nm (B), 475 nm (C), and 500 nm (D).

spectrum (Table 1). *P. marinus* CCMP 1986 showed a single peak at 687 nm with small shoulders at approximately 670 nm and 680 nm upon excitation of DV-Chl *a* at 445 nm (Fig. 2B). The second derivative spectrum resolved the main peak into two components located at 685.6 nm and 687.8 nm (Table 1). The shoulder observed at 680 nm was resolved to 680.4 nm. These peaks and wavelengths remained almost unchanged even by the excitation of DV-Chl *b* at 475 nm and of the carotenoids at 500 nm (Fig. 2C and D), indicating an efficient energy transfer from DV-Chl *b* and carotenoids to DV-Chl *a*. Upon excitation at 445 nm, a new component showed a fluorescence peak at 633 nm, possibly from an intermediate in DV-Chl biosynthesis. The typical PS II fluorescence at 695 nm and PS I fluorescence at approximately 725 nm was not detected, but we did observe a small band at approximately 700 nm. These spectra suggested a significant change(s) in the emission profile of *P. marinus*.

P. marinus CCMP 2773 and *P. marinus* CCMP 1375 produced fluorescence spectra with significant differences (Fig. 2B–D). The peak of the former was resolved into two component peaks at 679.6 nm and 689.0 nm by the second derivative spectra (Table 1), while the latter strain showed four peaks at 676.0 nm, 680.0 nm, 687.4 nm and 696.2 nm (Table 1). An emission from DV-Chl *b* was detected in *P. marinus* CCMP 2773 (Fig. 2C), suggesting an inefficient energy transfer from DV-Chl *b* to DV-Chl *a*. A very low intensity peak from DV-Chl *b* was also detected in *P. marinus* CCMP 1986 but not in *P. marinus* CCMP 1375.

Following the excitation of carotenoids at 500 nm (Fig. 2D), the fluorescence spectra in each of the three strains were almost identical to those excited either by DV-Chl *a* (Fig. 2B) or DV-Chl *b* (Fig. 2C), indicating a transfer of energy from the carotenoid(s) to DV-Chl *a*. However, carotenoid excitation did not sensitize fluorescence from DV-Chl *b*, which was detected even by magnified spectra (data not shown). Thus, a direct transfer of energy from the carotenoids to Chl *a* was revealed, and this situation was maintained in the three strains of *P. marinus*.

At physiological temperatures, the fluorescence spectra for the three strains of *P. marinus* were repetitive with respect to their peaks upon excitation of DV-Chl *a* (see Fig. S2 in Supporting Information). *P. marinus* CCMP 1986 showed a relatively wide peak in the range of 676 nm to 680 nm, on the other hand, *P. marinus* CCMP 2773 and *P. marinus* CCMP 1375 showed maximum peaks at 677 nm and 678 nm, respectively. These two strains showed an asymmetric band shape, with a wider band in the short-wavelength region, and a peak of significant intensity at approximately 655 nm originating from DV-Chl *b*. This was interpreted to mean that a thermal equilibrium between DV-Chl *a* and DV-Chl *b* was established at physiological temperatures; therefore, emission from a pigment at a higher-energy level was observed.

3.5. Excitation spectra

When fluorescence was monitored at the vibrational band of the main peak at 77 K, each of the three *P. marinus* strains exhibited excitation spectra with three peaks representing DV-Chl *a* and DV-Chl *b* in the blue region, although the relative intensities of the three bands were variable (see Fig. S3 in Supporting Information). The excitation spectra were, in general, similar to the absorption spectra at 80 K (Fig. 2A). Multiple components were resolved within the DV-Chl *a* and DV-Chl *b* bands, reflecting several absorption and fluorescence components. Peaks for carotenoids were located at wavelengths longer than 500 nm (see Fig. S3 in Supporting Information) and somewhat longer than those observed in *Synechocystis* (data not shown).

3.6. Time-resolved fluorescence spectra (TRFS)

Each TRFS was measured by excitation at 425 nm. The *Synechocystis* WT reflected the steady-state fluorescence spectrum (Fig. 1B–D), and a time-dependent shift of the maxima from the phycobiliproteins to PS I Chl *a* was clearly resolved [28]. On the other hand, the DV-Chl *a* *Synechocystis* mutant showed a lower PS I fluorescence spectrum, similar to the steady-state spectrum, in which relative intensity of the PS II fluorescence at 685 nm in the *Synechocystis* WT fluorescence is higher than that at 687 nm in the DV-Chl *a* *Synechocystis* mutant fluorescence (Fig. 1B–D).

At room temperature, *P. marinus* CCMP 1986, the high-light adapted strain, showed a relatively wide spectrum with a symmetric shape throughout the measuring time, which lasted for several ns (Fig. 3A). Excitation at 425 nm resulted in a maximum peak at 682 nm, and then at 100 ps after the excitation, the peak shifted

Table 1
Absorption and fluorescence peaks in the Qy bands of DV-Chl *a* in three strains of *P. marinus*.

Strains	Absorption peaks (nm)					
CCMP 1986			669.0	678.5	686.0	699.5
CCMP 2773	650.0	657.5	670.0	676.0	685.0	700.0
CCMP 1375		655.0		674.0	683.5	700.5
Strains	**Fluorescence peaks (nm)**					
CCMP 1986	673.0		680.4	685.6	687.8	
CCMP 2773			679.6		689.0	
CCMP 1375	676.0		680.0		687.4	696.2

Spectra were measured at 77 K and peaks were resolved by the second derivative spectra. For the fluorescence, the excitation wavelength was 445 nm.

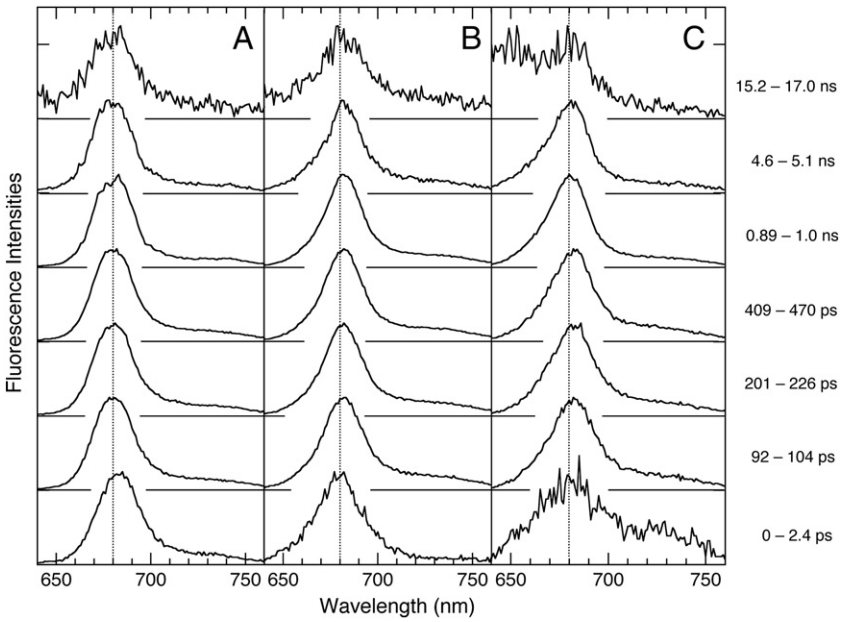

Fig. 3. Time-resolved fluorescence spectra (TRFS) for three strains of *P. marinus* at room temperature. (A) CCMP 1986, (B) CCMP 2773, and (C) CCMP 1375. Spectra were normalized to the maximum intensity of an individual spectrum. Vertical lines locate at 680 nm.

towards the blue region (680 nm), while the intensity in the wavelength region around 700 nm was slightly lower than that observed just after excitation. This reduction in intensity suggested the presence of a rapidly decaying component in this wavelength region in the initial time period. The spectra at 100 ps remained unchanged for over 2 ns. A wide bandwidth indicated the presence of multiple spectral components and thermal equilibrium between Chl *a* molecules with different transition energies, even though these components were not resolved by this TRFS.

In contrast, the TRFS of *P. marinus* CCMP1986 at 77 K (Fig. 4A) were very different from those observed at room temperature (Fig. 3A). The spectral changes were characterized by at least three features: (1) a time-dependent red-shift in the maximum for up to 17.0 ns after excitation, (2) sharpening of the spectral band shape in the initial time region, and (3) the appearance of a new band in the short-wavelength region of the maximum a long time after excitation. The maximum was observed at 683 nm at 0 ps, at 686 nm at 470 ps, at 693 nm at 5.1 ns, and at 688 nm at 17.0 ns. This behavior was explained by changes in the relative intensities of multiple components; for example, the shift from 683 nm to 686 nm corresponded to the energy transfer between the antenna Chls, and the shift to 693 nm corresponded to the appearance of a slowly decaying component at

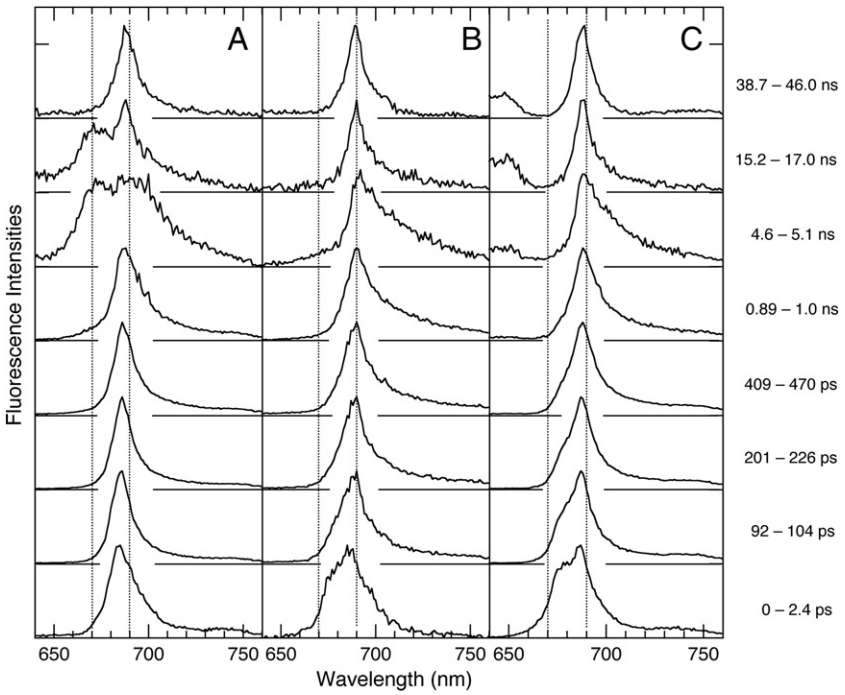

Fig. 4. Time-resolved fluorescence spectra (TRFS) for three strains of *P. marinus* at 77 K. (A) CCMP 1986, (B) CCMP 2773, and (C) CCMP 1375. Spectra were normalized to the maximum intensity of an individual spectrum. Vertical lines locate at 670 and 690 nm.

693 nm. A blue shift from 693 nm to 688 nm indicated the presence of delayed fluorescence (DF) from PS II at the shorter wavelength. Sharpening of the spectral band shape was also explained by a decrease in the relative intensity of the component with a maximum shorter than the apparent maximum; the lifetime of this component was short, suggesting a fast energy transfer from this component to the component responsible for the main fluorescence band. The appearance of a new component in the short-wavelength region of the maximum indicated the presence of an uncoupled component in the energy transfer sequence; the lifetime of this uncoupled component was relatively long; therefore, this component was observed for a long time after excitation.

P. marinus CCMP 2773, one of the low-light adapted strains, showed simple changes in peak locations and bandwidths, i.e., a full width at the half maximum (FWHM) at room temperature (Fig. 3B). At 0 ps, the peak was located at 680 nm with a FWHM of 30 nm. These two indices changed with time: at 104 ps, 682 nm and 26 nm; at 470 ps, 682 nm and 24 nm; at 1.0 ns, 682 nm and 23 nm; at 5.1 ns, 682 nm and 23 nm; and at 17.0 ns, 680 nm and 35 nm. The peak was continuously shifted to the red and the bandwidth changed for up to 5.1 ns. During the initial stage, a short-lived component was located in the short-wavelength region of the maximum, while a long-lived component appeared in the short-wavelength region of the maximum after measurements over a longer time period.

On the other hand, the TRFS at 77 K for *P. marinus* CCMP 2773 (Fig. 4B) was different from those observed at room temperature (Fig. 4A). The emission from the 675-nm antenna Chls was observed during the early time period. The spectral band changes were characterized by the following four features: (1) a red-shift of the maximum for up to 17.0 ns after excitation; (2) sharpening of the spectral band shape in the time up to 17.0 ns; (3) disappearance of the band in the short-wavelength region of the maximum during the initial time period; and (4) the appearance of a new band in the long-wavelength region of the maximum a few ns after excitation. The peak wavelengths were 688 nm at 0 ps; 689 nm at 226 ps; 689 nm at 470 ps; 691 nm at 5.1 ns; and 689 nm at 17.0 ns. These variations reflected changes in the relative intensities of multiple components. This phenomenon was also confirmed by changes in the bandwidth: 24 nm at 0 ps; 16 nm at 226 ps; 16 nm at 470 ps; 27 nm at 5.1 ns; and 12 nm at 17.0 ns. At 0 ps, a second band was clearly observed at 680 nm; however, it disappeared in approximately 600 ps. After this time, the relative intensity in the wavelength region longer than 700 nm increased but a new band did not appear. A cryptic component was present in this wavelength region; however, it was not resolved by TRFS. During the long time period after 5 ns, the bandwidth narrowed and the maximum shifted to the blue wavelength with time, indicating the presence of a band coming from delayed fluorescence. In the time period after 17.5 ns, DF was only one source for emission.

The TRFS for *P. marinus* CCMP 1375 (Figs. 3C and 4C), the second low-light adapted strain, were essentially similar to those observed for *P. marinus* CCMP 2773 (Figs. 3B and 4B). By looking closely at the TRFS at room temperature (Fig. 3C), we detected a very short-lived component whose maximum was located at approximately 650 nm. This corresponded to rapidly decaying DV-Chl *b*, responsible for the energy transfer to DV-Chl *a*. At 0 ps, the peak location and FWHM were 681 nm and 31 nm, respectively. These two measurements changed with time as follows: at 104 ps, 682 nm and 26 nm; at 47 ps, 682 nm and 26 nm; at 1.0 ns, 681 nm and 25 nm; at 5.1 ns, 681 nm and 27 nm; and at 17.0 ns, 681 nm and 49 nm. The band shape was asymmetric, and the bandwidth was always wider in the short-wavelength region, indicating the presence of a high-energy component(s). The component appearing during the initial time period might have a peak at approximately 665 nm, coming from DV-Chl *a*. At 650 nm, a long-lived component was observed, which resulted from uncoupled DV-Chl *b*.

At 77 K, the TRFS of *P. marinus* CCMP 1375 (Fig. 4C) were similar to those observed for *P. marinus* CCMP 2773 (Fig. 4B). In the initial time period, two peaks were observed at 677 nm and 687 nm. The former, a rather long-lived component, remained for up to 1.0 ns; this component was detected in each of the three strains, but was more evident in the low-light adapted species. The latter remained for up to 17.0 ns with a slight shift in location. The relative intensity in the wavelength region longer than 700 nm increased at the 1 ns time point, and lasted for up to 17.0 ns, suggesting the presence of a cryptic component in this region. At 17.0 ns, a sharp band was observed with a peak at 688 nm, corresponding to DF. The main peak shifted slightly with time; it was initially observed at 687 nm, and shifted to 688 nm by 104 ps, 689 nm at 5.1 ns, and 688 nm at 17.0 ns. A very long-lived component was observed at 650 nm, probably coming from uncoupled DV-Chl *b*.

To reveal transient fluorescence components and examine presence of the PS II 696-nm component and the PS I longer-wavelength component, we carried out global analysis for TRFS of *P. marinus* at 77 K. Each data set of fluorescence rise and decay curves ($F(\lambda, t)$) was fitted by a sum of exponentials with the common lifetime (τ_n) [29].

$$F(\lambda, t) = \sum_n A_n(\lambda)\exp\left(-\frac{t}{\tau_n}\right) \quad (1)$$

$A_n(\lambda)$ gives a fluorescence decay-associated spectrum (FDAS) of the *n*th lifetime (τ_n) component. To obtain FDAS, common lifetimes were adopted for three strains, and six lifetime components were required: 15 ps, 130 ps, 560 ps, 1.8 ns, 5.0 ns, and longer than 10 ns (Fig. 5).

The longest lifetime component mainly contributes to DF, which exhibited a maximum at 688 nm in FDAS. In the longest lifetime component of *P. marinus* CCMP 1375, additional bands were recognized in the shorter wavelength region (Fig. 5C). The origin of these bands is not clear, but most probably due to uncoupled pigment (s) in energy transfer sequence. In FDAS, coupling of negative and positive bands is a clear indication of energy transfer from the pigments giving the positive band to those giving the negative band. The 15-ps components exhibited negative and positive bands around 675 nm and 685–690 nm, respectively, indicating energy transfer from the 675-nm antenna Chls to the lower energy Chls. In the FDAS of *P. marinus* CCMP 2773 and CCMP 1375, the positive band showed a long tail to the shorter wavelength, but any peak which could be assigned due to DV-Chl *b* was not recognized. This indicates that energy transfer from DV-Chl *b* to DV-Chl *a* is an ultrafast process as is the case for the energy transfer from MV-Chl *b* to MV-Chl *a* in LHC II of land plant *Arabidopsis thaliana* [30] and in chloroplast of green alga *Codium fragile* [31].

The profiles of FDAS were different from each other, indicating multiple components in energy transfer sequence. The 673.0-nm, 680.4-nm, 685.6-nm, and 687.8-nm peaks found in the fluorescence spectrum of *P. marinus* CCMP 1986 (Table 1) are recognized as a positive peak in the 15-ps component, a shoulder at blue side of a maximum in the 130-ps component, a negative peak in the 15-ps component and the maximum in the 130-ps component, and a maximum in the 560-ps component, respectively (Fig. 5A). For the fluorescence peaks of *P. marinus* CCMP 2773 and CCMP 1375 (Table 1), the corresponding shoulder(s) or peak(s) are found in FDAS (Fig. 5B and C). The presence of a 696-nm component was suggested by the 1.8-ns components of all three strains and the 5.0-ns components of *P. marinus* CCMP 2773 and CCMP 1375 (Fig. 5). Although some FDAS exhibited a long tail towards longer wavelength, the PS I component was not clearly resolved.

3.7. Fluorescence decay curves at 77 K and delayed fluorescence

As shown for the TRFS of the three strains at 77 K (Fig. 4), DF was clearly observed at 688 nm towards the end of the measurement time

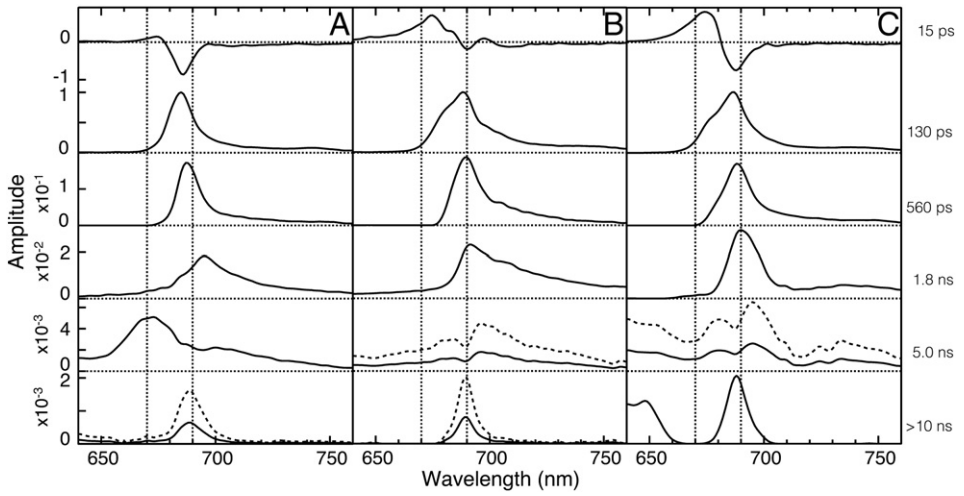

Fig. 5. Fluorescence decay-associated spectra (FDAS) for three strains of *P. marinus* at 77 K. (A) CCMP 1986, (B) CCMP 2773, and (C) CCMP 1375. Spectra were normalized to the maximum intensity of an individual 130 ps component spectrum. Dotted spectra indicate magnified amplitudes by a factor of 2.5. Vertical lines locate at 670 and 690 nm.

period. The DF bandwidth (FWHM) was almost constant among the strains and, at approximately 12 nm, relatively narrow. The DF lifetimes were estimated by convolution calculations of the fluorescence decay curves (Fig. 6), and the lifetimes and amplitudes are summarized in Table 2. The lifetimes for DF varied slightly depending on the strain of *P. marinus*; however, the average lifetime was approximately 29 ns. This value was a little longer than for the DF observed for intact cells of other cyanobacteria; for example, 15 ns for *Synechocystis* [28], 18 ns for *Gloeobacter violaceus* PCC 7421 (Mimuro and Akimoto, unpublished data), and 15 ns for the Chl *d*-containing cyanobacterium *Acaryochloris marina* MBIC 11017 [23]. DF was suppressed for the *Synechocystis* mutant [22] and for an *Arabidopsis* mutant [32] whose Chl *a* was replaced with DV-Chl *a*. Thus, we observed striking differences in the photochemical reactions of PS II in systems with a replaced pigment, the *Synechocystis* mutant, compared to those with a natural pigment, the three strains of *P. marinus*.

4. Discussion

4.1. An explanation for the unique fluorescence properties observed in P. marinus

We found clear differences in the fluorescence properties between the low-light adapted strains (CCMP 1375 and CCMP 2773) and the high-light adapted strain (CCMP 1986) of *P. marinus*. The steady-state spectra at room temperature differed in their peak locations and in the contribution of the short-wavelength component, DV-Chl *b* (see Fig. S2 in Supporting Information). In the low-light adapted cells, a high-intensity peak from DV-Chl *b* was observed, and this was attributed to the thermal equilibrium between DV-Chl *a* and DV-Chl *b*. Equilibrium between Chl *a* and Chl *b* is observed in the Chl *a*/*b* antenna system, and it also occurs in the light-harvesting complex II (LHC II) found in plants and photosynthetic bacteria [33]. Although *P. marinus* do not contain complexes corresponding to LHC II, these complexes are replaced by the Prochlorophyte Chl *a*/*b* binding proteins (Pcbs), which belongs to CP43′ protein. It is known that CP43′ proteins are associated with PS I [20,34–36]; however, they are also reported to be associated with PS II [35]. If the Pcb complexes contain both DV-Chl *a* and DV-Chl *b*, an equilibrium can be expected within Pcb and/or between Pcb and the PS II core complexes. The number of genes responsible for the Pcb components differs in the three strains of *P. marinus* [37], and the association of Pcb components and the energy migration within an antenna system would be an interesting subject for further study.

Differences were also observed in the TRFS at room temperature. After thermal equilibrium was established, the peak positions of DV-Chl *a* fluorescence in the two low-light adapted strains were located at longer wavelengths than in the high-light adapted strain (Fig. 3). This suggested that the high-light adapted strain contains a greater amount of DV-Chl *a* with a higher transition energy than the low-light adapted strains, in which the higher-energy DV-Chl *a* might be mainly replaced by DV-Chl *b*.

At 77 K, *Synechocystis* WT exhibited PS II fluorescence bands at 685 and 696 nm (Fig. 1B and C), which were assigned to fluorescences from the core complexes, CP43 and CP47. On the other hand, the major fluorescence band was observed at approximately 687 nm in all three strains of *P. marinus* (Fig. 2B–D). This peak location was also induced by the replacement of MV-Chl *a* with DV-Chl *a* in the

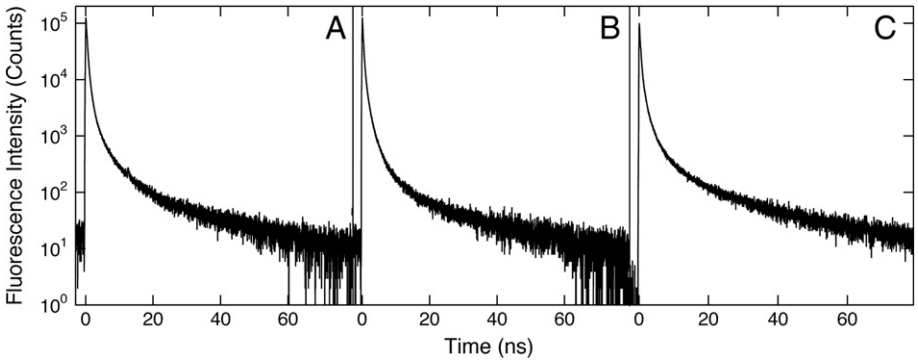

Fig. 6. Fluorescence decay curves for three strains of *P. marinus* at 77 K. (A) CCMP 1986, (B) CCMP 2773, and (C) CCMP 1375. Decay was monitored at 688 nm.

Table 2
Kinetic parameters of fluorescence decays at 688 nm in the three strains of *P. marinus* at 77 K.

Component	Lifetime (Amplitude)		
	CCMP 1986	CCMP 2773	CCMP 1375
τ_1 (A_1)	251 ps (0.749)	175 ps (0.756)	148 ps (0.576)
τ_2 (A_2)	618 ps (0.219)	525 ps (0.200)	422 ps (0.367)
τ_3 (A_3)	1.98 ns (0.027)	1.48 ns (0.040)	1.63 ns (0.051)
τ_4 (A_4)	6.27 ns (0.004)	4.82 ns (0.004)	6.08 ns (0.005)
τ_5 (A_5)	30.7 ns (0.001)	28.4 ns (0.001)	29.0 ns (0.001)

Fluorescence decay curves were measured at 77 K. τ and A represent the lifetime and amplitude of individual fluorescence decay components, respectively, and were obtained by a convolution calculation. The fifth component (τ_5, A_5) corresponds to delayed fluorescence.

Synechocystis mutant (Fig. 1–D), leading to the idea that DV-Chl *a* is responsible for this peak shift. A band corresponding to PS II fluorescence at 696 nm was not observed; however, the presence of this component was strongly suggested by the TRFS data (Fig. 4) and the FDAS data (Fig. 5). In this sense, the PS II fluorescence properties of the three strains of *P. marinus* were not altered significantly, but showed modifications in the energy transfer to the 696-nm component. Several fluorescence bands were clearly detected in the short-wavelength region of the maxima in *P. marinus* (Fig. 2B–D and Table 1), indicating an inefficient transfer of energy between the antenna components, a property unique to *Prochlorococcus*. In addition, we noticed that the 696-nm component of DV-Chl *a*-containing *Synechocystis* showed lower intensity fluorescence when compared with MV-Chl *a*-containing *Synechocystis* (Fig. 1B–D). This indicated that replacement of MV-Chl *a* with DV-Chl *a* induced a shift in the emission maximum from 685 nm to 687 nm and a low transfer efficiency to the 696-nm component. These changes might be induced by changes in the interaction between DV-Chl *a* and a protein moiety, probably CP47.

The presence of a PS I fluorescence component was not resolved in *P. marinus*. Since the 80 K absorption spectra (Fig. 2A) clearly showed the presence of red Chl in the three strains, we would have expected fluorescence from this component. However, it was not detected even by the second derivative spectrum (Table 1). The TRFS for the three strains (between the time periods of 4.6–5.1 ns and 15.2–17.0 ns, Fig. 4) suggested the presence of a long-wavelength component; however, it was not hard to expect that the maximum was located at a wavelength longer than 720 nm in FDAS (Fig. 5). TRFS can detect the presence of even an intermediary component; however, the presence of a PS I fluorescence component was not clearly shown. This data supported previous studies, which have reported the absence of PS I fluorescence in *Gloeobacter violaceus* PCC 7421 [38] and, at the same time, suggested that red Chls in *P. marinus* were not responsible for the long-wavelength emission observed.

A fairly long lifetime for antenna fluorescence at 77 K (Table 2) might correlate with an adaptation to high-light conditions. In *P. marinus* CCMP 1986, the lifetimes of the two main decay components were longer than those in the other two strains (Table 2), indicating less efficient energy transfer in the antenna system, even though DV-Chl *b* was less abundant. This could be interpreted to mean that a large input of excitation energy to the photochemical system is regulated through the efficiency of energy transfer. This hypothesis raises a new aspect in the adaptation of *Prochlorococcus* to different light conditions.

4.2. Changes in charge recombination after pigment replacement

DF is one of the indices of the energy level of the reaction center complexes in PS II. DF was suppressed for the DV-Chl *a*-containing *Synechocystis* sp. [22], but was seen in the three strains of *P. marinus* (Fig. 7 and Table 2). Therefore, DV-Chl *a* itself has an ability to function as a proper primary electron donor in the PS II reaction center. Upon the exchange of a pigment, the optimization processes need to occur in the protein moieties of PS II. It is possible that the optimization process involves stabilization of the photochemical reaction, realized at the level of the reaction center proteins, D1 and D2. DF and singlet oxygen formation are competitive reactions in terms of the dissipation of the excited energy after charge recombination, and it is possible that the latter might be connected with damage of photosynthesis and critical for cell survival. In an acetone solution, the yield of singlet oxygen from DV-Chl *a* is approximately 20% higher than from MV-Chl *a* [15], and the same tendency has been observed for PS II complexes (Tomo et al., unpublished data). DF was suppressed in the mutated *Synechocystis*, but significant DF in *P. marinus* clearly indicated differences in the optimization process for energy dissipation after charge recombination.

The difference in singlet oxygen formation or in DF might be related to amino acid(s) replacement in the D1 and/or D2 proteins. Specific changes were observed at several loci in the D1 and D2 protein sequences from *P. marinus* (Fig. 7). At amino acid 206, which is located in the D helix of the D1 protein from *P. marinus*, and which corresponds to amino acid 205 in *Synechocystis*, valine was substituted with methionine. This substitution might have some effect on the photochemical reaction. Additionally, a glycine to cystein substitution was found at amino acid 282 located in the E helix. Similarly, in the D2 protein, the substitution with glutamine at the amino acid 218 was observed (Fig. 7). Furthermore, a seven amino acid insertion observed between the D helix and DE helix in the D2 proteins of *P. marinus* CCMP 1986 and CCMP 1375 might induce additional changes. At the present stage, it is not clear which residue(s) affect electron transfer process in D1/D2 protein. However, it is expected that a few substitution of residues can optimize the electron transfer system containing DV-Chl, since the number of residues conserved only among three strains of *P. marinus* is small (Fig. 7).

Recently, Ito et al. (2008) created a knockout mutant of *Synechocystis* by disrupting the gene essential for the reduction of 8-vinyl group of DV-protochlorophyllide *a* [5]. The mutant accumulated DV-Chl *a* instead of MV-Chl *a*; furthermore, cells were not stable under high-light conditions, and their pigments bleached within 1 day. This was interpreted to mean that the protein environments had not been altered by amino acid substitutions to optimize the pigment–protein and protein-protein interactions for the newly acquired pigment in the mutant. In line with this observation, DF was suppressed in the transformant [22]; on the other hand, the presence of DF was confirmed in the three strains of *P. marinus* in this study (Figs. 4–6). This clearly indicated that DV-Chl *a* itself did not induce an unstable reaction system, but that optimization of the system might not be established in the *Synechocystis* transformant.

Photochemical reactions were highly sensitive to high-light treatments in the *Synechocystis* mutant. Specifically, DV-Chl *a* was rapidly bleached under high-light conditions, and significant dissociation of complexes and degradation of D1 proteins was detected [22]. In *P. marinus*, a low-light adapted strain has evolved to a high-light adapted strain. As indicated by the results from this study, differences in energy transfer times (Table 2) and/or the fluorescence spectra at room temperature (see Fig. S2 in Supporting Information) are typical examples of the progression from a low-light adapted species to a high-light adapted species. With this in mind, it is possible that similar evolutionary process(es) take place continuously. The replacement of the MV-Chl *a* pigment with DV-Chl *a* was accomplished by the loss of a gene for 3,8-divinyl protochlorophyllide *a* 8-vinyl reductase [4]; however, optimization of the reaction system(s) with the modified pigments requires further modifications of the proteins involved in the reactions.

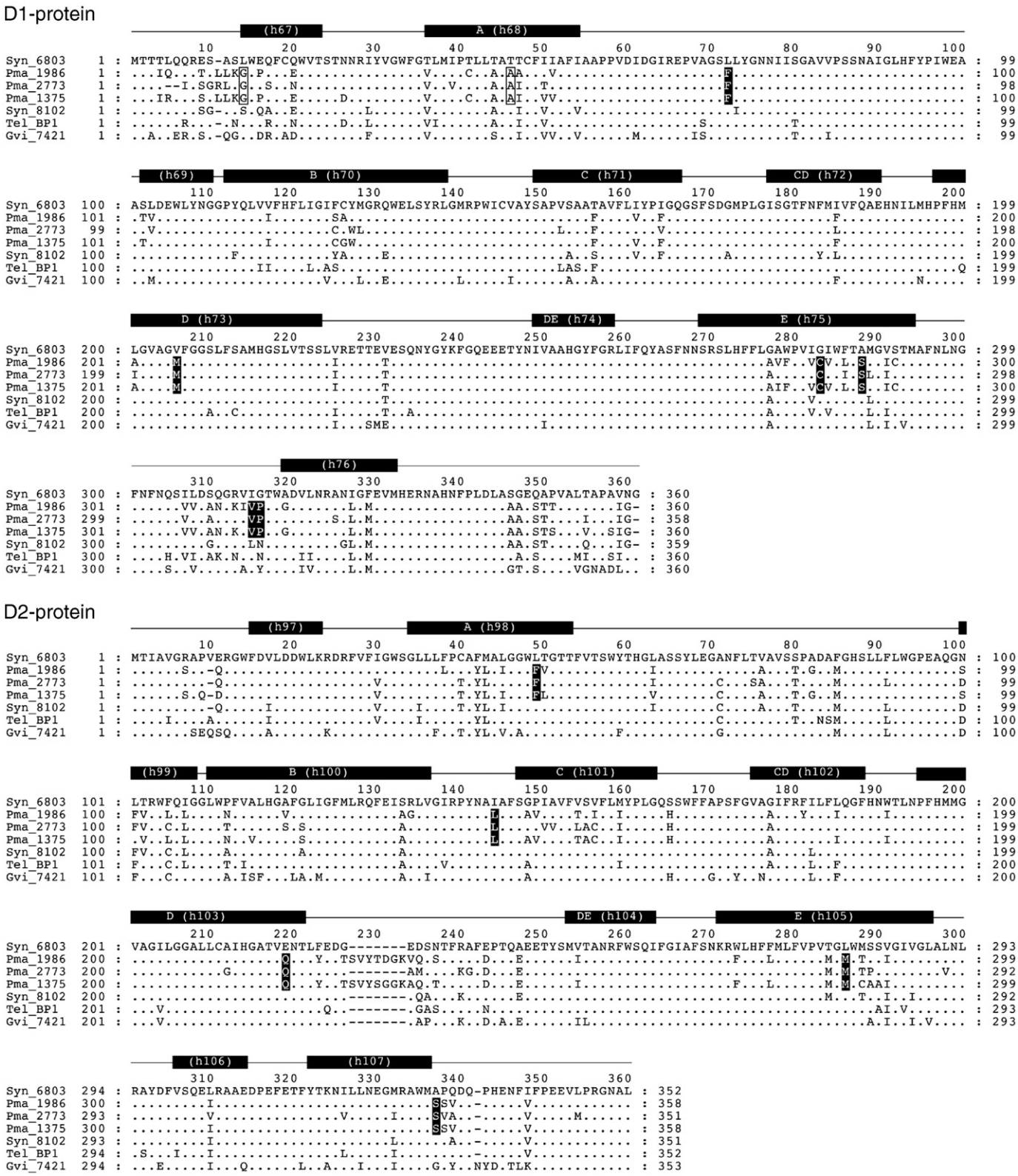

Fig. 7. Alignment of amino acid sequences for D1 and D2 proteins from several cyanobacterial species. Cyanobacteria from top to bottom: *Synechocystis* sp. PCC 6803, *P. marinus* CCMP 1986, *P. marinus* CCMP 2773, *P. marinus* CCMP 1375, *Synechococcus* sp. WH8102, *Thermosynechococcus elongates*, and *Gloeobacter violaceus* PCC 7421. The amino acids conserved only among three strains of *P. marinus* are boxed. Among them, the amino acids conserved among 12 sequenced strains of *P. marinus* are highlighted in reverse contrast.

4.3. Changes in energy transfer processes after pigment replacement

Differences in the fluorescence spectra between DV-Chl *a*-replaced *Synechocystis* (Fig. 1B-D) and *P. marinus* (Fig. 1B–D) were a reflection of the diversity in the energy transfer processes. The *Synechocystis* transformant showed an essentially identical fluorescence spectrum in Chl-fluorescence region to that of *Synechocystis*, i.e., three peaks at 685 nm, 696 nm and 724 nm at 77 K (Fig. 1B and C). In contrast, as

shown in this study, the three strains of *P. marinus* produced only one fluorescence band at approximately 687 nm (Fig. 2B–D). This indicated that replacement of a pigment did not induce an alteration in the antenna system as evidenced by differences in the fluorescence bands of PS II. A shift in the fluorescence maximum from 685 nm to 687 nm and a low energy transfer efficiency to the 696-nm component were commonly observed both in the *Synechocystis* mutant and *P. marinus*; however, an inefficient energy transfer in the Chl antenna in *P. marinus* suggests that intermolecular interaction (s) between DV-Chls and/or between DV-Chl and proteins should not be necessarily optimized for the energy transfer to the 696-nm component. Further change(s) will extend to the PS I complexes (PsaA and PasB) for an overall energy transfer and energy distribution between the two photosystems. Even though the presence of the red Chls was observed in absorption spectra of *P. marinus* (Fig. 2A), PS I fluorescence was not detected at all (Fig. 4). Although the reason for the absence of a PS I fluorescence band is not yet clear, one explanation is a very fast energy transfer [39]. The absence of PS I fluorescence favors energy utilization at physiological temperatures. It is known that even at physiological temperatures, PS I fluorescence is observed with a low efficiency [40]. If PS I fluorescence is completely absent, its energy will be transferred to the antenna complexes, including PS II, due to the thermal equilibrium between the antenna, resulting in the efficient utilization of energy by the two photosystems.

We examined optical properties of DV-Chl *a*-containing cyanobacteria, a *Synechocystis* mutant and three strains of *P. marinus*. Replacement of MV-Chl with DV-Chl caused changes in transition energies (Fig. 1). In this sense, the absorption spectra reflected the replacement of pigment for the *Synechocystis* mutant (Fig. 1A) and *P. marinus* (Fig. 2A) both. On the other hand, fluorescence spectra exhibited different properties, which cannot be explained only by the replacement. Compared with the fluorescence behaviors of the *Synechocystis* mutant, *P. marinus* fluorescence exhibited three characteristic properties: (1) DF was clearly observed, (2) the 696-nm band was not resolved in the steady-state fluorescence but was recognized by TRFS, and (3) the PS I fluorescence was absent even in the TRFS. The electron transfer and energy transfer are intermolecular processes and sensitive to molecular environment. Therefore, the above differences in fluorescence properties should originate from differences in interactions between DV-Chls and/or between protein and DV-Chl. By having DV-Chl as a major pigment, the *Synechocystis* mutant and *P. marinus* absorb light energy that MV-Chl cannot capture. This is advantageous for light harvesting. However, to achieve electron transfer and energy transfer in the same way as established in the *Synechocystis* WT, it might be necessary to optimize molecular interactions including DV-Chl(s). Analysis of the optimization process(es) of molecular environment that occur upon replacement of pigment species should be required and expanded to an analysis of the evolutionary process(es) from anoxygenic photosynthetic bacteria to cyanobacteria in the future.

Supplementary materials related to this article can be found online at doi:10.1016/j.bbabio.2011.02.011.

Acknowledgements

The authors would like to thank Ms. H. Uchida, Kobe University, for maintenance of the *Prochlorococcus* cultures and Prof. A. Tanaka, Hokkaido University, for his kind gift of the *Synechocystis* mutant. This study was supported by a Grant-in-Aid for Creative Scientific Research (17GS0314) to MM and AM from the Japanese Society for the Promotion of Science (JSPS), by a Grant-in-Aid for scientific research from MEXT to T. Tomo (21570038) and to MM (22370017), by the Special Coordination Funds for Promoting Science and Technology. and by a Grant-in-Aid to S.A. from the Creation of Innovation Centers for Advanced Interdisciplinary Research Areas (Innovative Bioproduction Kobe) programs of MEXT.

References

[1] S.W. Chisholm, S.L. Frankel, R. Goericke, R.J. Olson, B. Palenik, J.B. Waterbury, L. West-Johnsrud, E.R. Zettler, *Prochlorococcus marinus* nov. gen. nov. sp.: an oxyphototrophic marine prokaryote containing divinyl chlorophyll *a* and *b*, Arch. Microbiol. 157 (1992) 297–300.
[2] G. Rocap, F.W. Larimer, J. Lamerdin, S. Malfatti, P. Chain, N.A. Ahlgren, A. Arellano, M. Coleman, L. Hauser, W.R. Hess, Z.I. Johnson, M. Land, D. Lindell, A.F. Post, W. Regala, M. Shah, S.L. Shaw, C. Steglich, M.B. Sullivan, C.S. Ting, A. Tolonen, E.A. Webb, E.R. Zinser, S.W. Chisholm, Genome divergence in two *Prochlorococcus* ecotypes reflects oceanic niche differentiation, Nature 424 (2003) 1042–1047.
[3] C.S. Ting, G. Rocap, J. King, S.W. Chisholm, Cyanobacterial photosynthesis in the oceans: the origins and significance of divergent light-harvesting strategies, Trends Microbiol. 10 (2002) 134–142.
[4] N. Nagata, R. Tanaka, S. Satoh, A. Tanaka, Identification of a vinyl reductase gene for chlorophyll synthesis in *Arabidopsis thaliana* and implications for the evolution of Prochlorococcus species, Plant Cell 17 (2005) 233–240.
[5] H. Ito, M. Yokono, R. Tanaka, A. Tanaka, Identification of a novel vinyl reductase gene essential for the biosynthesis of monovinyl chlorophyll in *Synechocystis* sp. PCC6803, J. Biol. Chem. 283 (2008) 9002–9011.
[6] M.R. Islam, S. Aikawa, T. Midorikawa, Y. Kashino, K. Satoh, H. Koike, *slr1923* of *Synechocystis* sp. PCC6803 is essential for conversion of 3,8-divinyl(proto) chlorophyll(ide) to 3-monovinyl(proto)chlorophyll(ide), Plant Physiol. 148 (2008) 1068–1081.
[7] R. Tanaka, A. Tanaka, Tetrapyrrole biosynthesis in higher plants, Annu. Rev. Plant Biol. 58 (2007) 321–346.
[8] A. Bricaud, K. Allali, A. Morel, D. Marie, M.J.W. Veldhuis, F. Partensky, D. Vaulot, Divinyl chlorophyll *a*-specific absorption coefficients and absorption efficiency factors for *Prochlorococcus marinus*: kinetics of photoacclimation, Mar. Ecol. Prog. Ser. 188 (1999) 21–32.
[9] M.D. DuRand, R.J. Olson, S.W. Chisholm, Phytoplankton population dynamics at the Bermuda Atlantic Time-series station in the Sargasso Sea, Deep Sea Res. II 48 (2001) 1983–2003.
[10] F. Partensky, L. Garczarek, *Prochlorococcus*: advantages and limits of minimalism, Annu. Rev. Mar. Sci. 2 (2010) 305–331.
[11] C.S. Ting, M.E. Ramsey, Y.L. Wang, A.M. Frost, E. Jun, T. Durham, Minimal genomes, maximal productivity: comparative genomics of the photosystem and light-harvesting complexes in the marine cyanobacterium, *Prochlorococcus*, Photosynth. Res. 101 (2009) 1–19.
[12] F. Partensky, W.R. Hess, D. Vaulot, *Prochlorococcus*, a marine photosynthetic prokaryote of global significance, Microbiol. Mol. Biol. Rev. 63 (1999) 106–127.
[13] C.S. Ting, G. Rocap, J. King, S.W. Chisholm, Cyanobacterial photosynthesis in the oceans: the origins and significance of divergent light-harvesting strategies, Trends Microbiol. 10 (2002) 134–142.
[14] D.J. Scanlan, M. Ostrowski, S. Mazard, A. Dufresne, L. Garczarek, W.R. Hess, A.F. Post, M. Hagemann, I. Paulsen, F. Partensky, Ecological genomics of marine picocyanobacteria, Microbiol. Mol. Biol. Rev. 73 (2009) 249–299.
[15] S. Okazaki, T. Tomo, M. Mimuro, Direct measurement of singlet oxygen produced by four chlorin-ringed chlorophyll species in acetone solution, Chem. Phys. Lett. 485 (2010) 202–206.
[16] V.H.R. Schmid, Light-harvesting complexes of vascular plants, Cell. Mol. Life Sci. 65 (2008) 3619–3639.
[17] A. Dufresne, M. Salanoubat, F. Partensky, F. Artiguenave, I.M. Axmann, V. Barbe, S. Duprat, M.Y. Galperin, E.V. Koonin, F. Le Gall, K.S. Makarova, M. Ostrowski, S. Oztas, C. Robert, I.B. Rogozin, D.J. Scanlan, N.T. de Marsac, J. Weissenbach, P. Wincker, Y.I. Wolf, W.R. Hess, Genome sequence of the cyanobacterium *Prochlorococcus marinus* SS120, a nearly minimal oxyphototrophic genome, Proc. Natl. Acad. Sci. USA 100 (2003) 10020–10025.
[18] L.R. Moore, G. Rocap, S.W. Chisholm, Physiology and molecular phylogeny of coexisting *Prochlorococcus* ecotypes, Nature 393 (1998) 464–467.
[19] F. Partensky, J. La Roche, K. Wyman, P.G. Falkowski, The divinyl-chlorophyll *a*/*b*-protein complexes of two strains of the oxyphototrophic marine prokaryote *Prochlorococcus* – characterization and response to changes in growth irradiance, Photosynth. Res. 51 (1997) 209–222.
[20] L. Garczarek, G.W.M. van der Staay, J.C. Thomas, F. Partensky, Isolation and characterization of Photosystem I from two strains of the marine oxychlorobacterium *Prochlorococcus*, Photosynth. Res. 56 (1998) 131–141.
[21] L. Garczarek, W.R. Hess, J. Holtzendorff, G.W.M. van der Staay, F. Partensky, Multiplication of antenna genes as a major adaptation to low light in a marine prokaryote, Proc. Natl Acad. Sci. USA 97 (2000) 4098–4101.
[22] T. Tomo, S. Akimoto, H. Ito, T. Tsuchiya, M. Fukuya, A. Tanaka, M. Mimuro, Replacement of chlorophyll with di-vinyl chlorophyll in the antenna and reaction center complexes of the cyanobacterium *Synechocystis* sp. PCC 6803: characterization of spectral and photochemical properties, Biochim. Biophys. Acta 1787 (2009) 191–200.
[23] M. Mimuro, S. Akimoto, I. Yamazaki, H. Miyashita, S. Miyachi, Fluorescence properties of chlorophyll *d*-dominating prokaryotic alga, *Acaryochloris marina*: studies using time-resolved fluorescence spectroscopy on intact cells, Biochim. Biophys. Acta 1412 (1999) 37–46.
[24] M. Zapata, F. Rodriguez, J.L. Garrid, Separation of chlorophylls and carotenoids from marine phytoplankton: a new HPLC method using a reversed phase C8 column and pyridine-containing mobile phases, Mar. Ecol. Prog. Ser. 195 (2000) 29–45.

[25] R.J. Porra, W.A. Thompson, P.E. Kriedemann, Determination of accurate extinction coefficients and simultaneous equations for assaying chlorophylls *a* and *b* extracted with four different solvents: verification of the concentration of chlorophyll standards by atomic absorption spectroscopy, Biochim. Biophys. Acta 975 (1989) 384–394.
[26] K. Koyama, H. Suzuki, T. Noguchi, S. Akimoto, T. Tsuchiya, M. Mimuro, Oxygen evolution in the thylakoid-lacking cyanobacterium *Gloeobacter violaceus* PCC 7421, Biochim. Biophys. Acta 1777 (2008) 369–378.
[27] F. Partensky, N. Hoepffner, W.K.W. Li, O. Ulloa, D. Vaulot, Photoacclimation of *Prochlorococcus* sp. (Prochlorophyta) strains isolated from the North Atlantic and the Mediterranean Sea, Plant Physiol. 101 (1993) 285–296.
[28] M. Mimuro, S. Akimoto, T. Gotoh, M. Yokono, M. Akiyama, T. Tsuchiya, H. Miyashita, M. Kobayashi, I. Yamazaki, Identification of the primary electron donor in PS II of the Chl *d*-dominated cyanobacterium *Acaryochloris marina*, FEBS Lett. 556 (2004) 95–98.
[29] M. Yokono, S. Akimoto, K. Koyama, T. Tsuchiya, M. Mimuro, Energy transfer processes in *Gloeobacter violaceus* PCC 7421 that possesses phycobilisomes with a unique morphology, Biochim. Biophys. Acta 1777 (2008) 55–65.
[30] S. Akimoto, M. Yokono, M. Ohmae, I. Yamazaki, A. Tanaka, M. Higuchi, T. Tsuchiya, H. Miyashita, M. Mimuro, Ultrafast excitation relaxation dynamics of lutein in solution and in the light-harvesting complexes II isolated from *Arabidopsis thaliana*, J. Phys. Chem. B 109 (2005) 12612–12619.
[31] S. Akimoto, I. Yamazaki, A. Murakami, S. Takaichi, M. Mimuro, Ultrafast excitation relaxation dynamics and energy transfer in the siphonaxanthin-containing green alga *Codium fragile*, Chem. Phys. Lett. 390 (2004) 45–49.
[32] S. Akimoto, M. Yokono, M. Ohmae, I. Yamazaki, N. Nagata, R. Tanaka, A. Tanaka, M. Mimuro, Excitation energy transfer in the antenna system with divinyl-chlorophylls in the vinyl reductase-expressing *Arabidopsis*, Chem. Phys. Lett. 409 (2005) 167–171.
[33] K. Nakayama, M. Mimuro, Chlorophyll forms and excitation energy transfer pathways in light-harvesting chlorophyll *a*/*b* protein complexes isolated from the siphonous green alga, *Bryopsis maxima*, Biochim. Biophys. Acta 1184 (1994) 103–110.
[34] T.S. Bibby, J. Nield, F. Partensky, J. Barber, Antenna ring around photosystem I, Nature 413 (2001) 590.
[35] M. Chen, T.S. Bibby, Photosynthetic apparatus of antenna-reaction centres supercomplexes in oxyphotobacteria: insight through significance of Pcb/IsiA proteins, Photosynth. Res. 86 (2005) 165–173.
[36] Y. Zhang, M. Chen, W.B. Church, K.W. Lau, A.W.D. Larkum, L.S. Jermiin, The molecular structure of the IsiA–Photosystem I supercomplex, modelled from high-resolution, crystal structures of Photosystem I and the CP43 protein, Biochim. Biophys. Acta 1797 (2010) 457–465.
[37] M.L. Coleman, S.W. Chisholm, Code and context: *Prochlorococcus* as a model for cross-scale biology, Trends Microbiol. 15 (2007) 398–407.
[38] M. Mimuro, T. Ookubo, D. Takahashi, T. Sakawa, S. Akimoto, I. Yamazaki, H. Miyashita, Unique fluorescence properties of a cyanobacterium *Gloeobacter violaceus* PCC 7421: reasons for absence of the long-wavelength PSI Chl *a* fluorescence at – 196 °C, Plant Cell Physiol. 43 (2002) 587–594.
[39] M. Mimuro, M. Yokono, S. Akimoto, Variations in photosystem I properties in the primordial cyanobacterium *Gloeobacter violaceus* PCC 7421, Photochem. Photobiol. 86 (2010) 62–69.
[40] I. Yamazaki, M. Mimuro, N. Tamai, T. Yamazaki, Y. Fujita, Picosecond time-resolved fluorescence spectra of photosystem I and II in *Chlorella pyrenoidosa*, FEBS Lett. 179 (1985) 65–68.